Proceedings of the 2001 IEEE
International Conference on Robotics & Automation
Seoul, Korea • May 21-26, 2001

Fundamentals and Analysis of Compliance Characteristics for Multi-Fingered Hands

Byoung-Ho Kim°,†, Byung-Ju Yi°, Sang-Rok Oh†, and Il Hong Suh°

° : School of Electrical Eng. and Computer Science, Hanyang Univ., Seoul, Korea
† : Intelligent System Control Research Center, KIST, Seoul, Korea
(E-mail: bj@email.hanyang.ac.kr)

Abstract

In this paper, we provide a guideline for specifying compliance characteristics in the operational space of multi-fingered hands. Through the analysis of the stiffness relation between the operational space and the fingertip space of multi-fingered hands, it is shown that some of coupling stiffness elements cannot be planned arbitrary. And an independent finger-based compliance control method to achieve the given compliance characteristics is presented. Through the analytical results, it is concluded that the operational stiffness matrix should be carefully specified by considering the grasp geometry of multi-fingered hands for successful grasping and manipulation tasks and also three-dimensional compliance control can be achieved by five-fingered hands like human.

Keywords : *multi-fingered robot hand, independent finger-based compliance control, specifying compliance characteristics*

1 Introduction

Related to grasping and manipulation of object by using robot hands or multiple robot arms, many researchers have proposed explicit force-based control methods[1][2]-[8]. However, implementation of those methods may not be practically easy because it is not only hard to employ force sensors in finger mechanisms, but also problematic to successfully process noisy force signals. Also, the integration of tactile and force information for individual finger control, and the combination of information from different fingers to guide the hand action are not still well known[9]. Therefore, it has been pointed out that instead of employing force signals, stiffness or compliance as successful alternatives can be used for characterizing the grasping and manipulation of robot hands[10][11]. Specially, when an object grasped by multi-fingered hand is being manipulated in constrained space, the appropriate stiffness planning of the hand is very important for successful compliant tasks[12]-[14].

Many approaches have been reported in the field of grasp stiffness or compliance[15]-[21]. Shimoga[15] summarized the conventional grasp synthesis algorithms for robot hands. The stiffness of objects grasped by virtual springs was analyzed in cases of planar and three-dimensional space[16]. Yokoi, et al.[17] proposed a direct compliance control method and applied the method to a parallel arm. Cutkosky et al.[10] analyzed the effective grasp stiffness by considering the structural compliances in fingers and fingertips, servo gains at the joints of finger, and small changes in the grasp geometry that may affect the grasp forces acting upon the object. In [18], it is pointed out that a stiffness matrix containing some off-diagonal terms can be useful to prevent jamming of contact tasks. Li et al.[19] classified a grasp matrix into symmetric and anti-symmetric parts. An experimental investigation was performed for successful object stiffness control using multi-fingered robot hand[20]. Also, Kao, et al.[11] tried to apply stiffness models usually employed in robotics research to the analysis of human grasping behaviors. Recently, Kim, et al.[21] proposed an independent finger/joint-based compliance control method for robot hands manipulating an object, and also the geometric condition for successful implementation of compliance control scheme have been addressed. They showed that an independent finger/joint-based compliance control via redundant actuation was more adequate to modulate the operational stiffness comparing with the case of the kinematically redundant structured fingers or manipulators. Some researchers have investigated the task-based stiffness characteristics[22]-[24]. However, the methodology to achieve the desired stiffness characteristics is still an open research field.

In this paper, through analyzing the stiffness relation between the operational space and the fingertip space of multi-fingered hands, we provide a guideline for specifying compliance characteristics in the operational space of multi-fingered hands. Also, it is shown that the concept of compliance analysis is very useful for finding necessary finger condition of multi-fingered hands. And an independent finger-based compliance control method is presented to achieve the specified compliance characteristics.

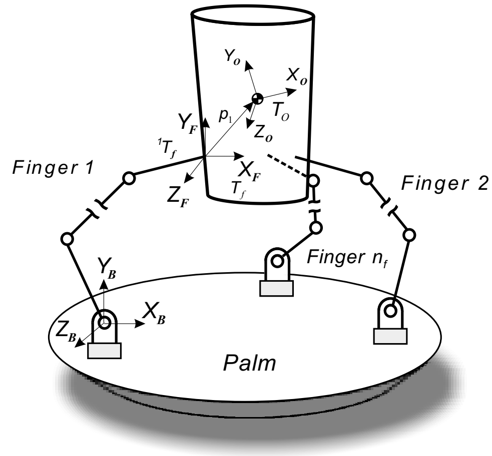

Figure 1: A multi-fingered robot hand.

2 Stiffness Relation of Multi-Fingered Hand

The stiffness or compliance can be employed for characterizing the grasping and manipulation of robot hands in the case that it is specially dominated in approximated linear analysis where low velocities and small relative motions lead to small inertial forces. In this section, we analyze the stiffness relation between the operational space and the fingertip space.

Consider a rigid object being manipulated by a n_f-fingered robot hand as shown in Figure 1, where each finger has ${}^in_j$-joints, and the relation between the generalized force vector in the operational space and the fingertip force vector is given by

$$T_o = [\boldsymbol{G}_o^f]^T T_f, \qquad (1)$$

where $T_o \in \mathcal{R}^{n\times 1}$ denotes the generalized force vector in the operational space including the inertial load and external load, the fingertip force vector $T_f \in \mathcal{R}^{m\times 1}$ in the fingertip space is expressed as

$$T_f = \left[\begin{array}{cccc} ({}^1T_f)^T & ({}^2T_f)^T & \cdots & ({}^{n_f}T_f)^T \end{array}\right]^T,$$

and the Jacobian matrix between the operational space and the fingertip space $[\boldsymbol{G}_o^f] \in \mathcal{R}^{m\times n}$ is given by

$$[\boldsymbol{G}_o^f] = \left[\begin{array}{cccc} [{}^1\boldsymbol{G}_o^f]^T & [{}^2\boldsymbol{G}_o^f]^T & \cdots & [{}^{n_f}\boldsymbol{G}_o^f]^T \end{array}\right]^T,$$

$$[{}^i\boldsymbol{G}_o^f] = \left[\begin{array}{cc} {}^f_o\boldsymbol{R}_i & {}^f_op_i \times {}^f_o\boldsymbol{R}_i \\ 0 & {}^f_o\boldsymbol{R}_i \end{array}\right].$$

Here, ${}^f_o\boldsymbol{R}_i$ and ${}^f_op_i$ denotes the rotation matrix and the position vector from the operational space to the fingertip space, respectively. Also, $m(m = \sum_{i=1}^{n_f} {}^in_{fp}$, where ${}^in_{fp}$ denotes the dimension of the ith fingertip) denotes the total dimension of wrenches applied to the grasped object by n_f fingers.

When the trajectory of the grasped object is prespecified, the task of load distribution will be the determination of the fingertip forces and moments in order to achieve a desired motion of the object and to maintain the grasp. The general solution of (1) is given by

$$T_f = ([\boldsymbol{G}_o^f]^T)^+ T_o + (\boldsymbol{I} - ([\boldsymbol{G}_o^f]^T)^+ [\boldsymbol{G}_o^f]^T)\xi_f, \qquad (2)$$

where the superscript T implies the transpose of a matrix, $([\boldsymbol{G}_o^f]^T)^+$ is a pseudo-inverse of $[\boldsymbol{G}_o^f]^T$, and ξ_f is an arbitrary $m \times 1$ vector. $\boldsymbol{I}$ denotes an $m \times m$ identity matrix.

According to (2), we need 3 fingers to control 6×1 operational force and 3×1 internal force vectors under the assumption that contact type is point contact with friction. However, the number of required fingers will be different for the case of compliance control.

Using (2), we can perform explicit force control of robot hands by using force sensor signal, but the fine finger motion control is practically hard because force measurement at the fingertip is not easy and the real force signal is very noisy. Therefore, stiffness or compliance control method can be usefully applied to robot hand instead of using explicit force control method and also, compliance control approach is believed to be more human-like.

By taking the partial derivative of (1) with respect to u_o, the $n \times n$ stiffness matrix in the operational space including the effect of the change of contact configuration can be expressed as follows :

$$[\boldsymbol{K}_o^{'}] = [\boldsymbol{G}_o^f]^T [\boldsymbol{K}_f][\boldsymbol{G}_o^f] - ([T_f]^T \circ [\boldsymbol{H}_{oo}^f]), \qquad (3)$$

and we define

$$[\boldsymbol{K}_o] = [\boldsymbol{K}_o^{'}] + ([T_f]^T \circ [\boldsymbol{H}_{oo}^f]) = [\boldsymbol{G}_o^f]^T[\boldsymbol{K}_f][\boldsymbol{G}_o^f], \quad (4)$$

where $[\boldsymbol{K}_f]$ representing the $m \times m$ stiffness matrix in the fingertip space is expressed as

$$[\boldsymbol{K}_f] = \begin{bmatrix} {}^1\boldsymbol{K}_f & {}^{12}\boldsymbol{K}_f & \cdots & {}^{1n_f}\boldsymbol{K}_f \\ {}^{21}\boldsymbol{K}_f & {}^2\boldsymbol{K}_f & \cdots & {}^{2n_f}\boldsymbol{K}_f \\ \vdots & \vdots & \ddots & \vdots \\ {}^{n_f1}\boldsymbol{K}_f & {}^{n_f2}\boldsymbol{K}_f & \cdots & {}^{n_f}\boldsymbol{K}_f \end{bmatrix},$$

in which representing ${}^i\boldsymbol{K}_f (i = 1, \cdots, n_f)$ is given by

$$[{}^i\boldsymbol{K}_f] = \begin{bmatrix} {}^i\boldsymbol{K}_{fxx} & {}^i\boldsymbol{K}_{fxy} & {}^i\boldsymbol{K}_{fxz} \\ {}^i\boldsymbol{K}_{fyx} & {}^i\boldsymbol{K}_{fyy} & {}^i\boldsymbol{K}_{fyz} \\ {}^i\boldsymbol{K}_{fzx} & {}^i\boldsymbol{K}_{fzy} & {}^i\boldsymbol{K}_{fzz} \end{bmatrix},$$

${}^{ij}\boldsymbol{K}_f$ denotes the inter-finger coupling stiffness matrix between the ith finger and the jth finger. The operator of $(\circ)$ and $[\boldsymbol{H}_{oo}^f]$ represent the Generalized Scalar Dot Product[25] and the second-order kinematic influence coefficient matrix which represents the change of $[\boldsymbol{G}_o^f]$ with respect to contact configuration[26], respectively.

Generally, the six-degree of freedom operational compliance characteristics of (4) can be expressed by

$$\begin{bmatrix} \boldsymbol{K}_{o11} & \boldsymbol{K}_{o1j} & \cdots & \boldsymbol{K}_{o16} \\ \boldsymbol{K}_{oi1} & \boldsymbol{K}_{oij} & \cdots & \boldsymbol{K}_{oi6} \\ \vdots & \vdots & \ddots & \vdots \\ \boldsymbol{K}_{o61} & \boldsymbol{K}_{o6j} & \cdots & \boldsymbol{K}_{o66} \end{bmatrix} = \begin{bmatrix} g_{11} & g_{1j} & \cdots & g_{16} \\ g_{k1} & g_{kj} & \cdots & g_{k6} \\ \vdots & \vdots & \ddots & \vdots \\ g_{m1} & g_{mj} & \cdots & g_{m6} \end{bmatrix}^T \begin{bmatrix} \boldsymbol{K}_{f11} & \boldsymbol{K}_{f1l} & \cdots & \boldsymbol{K}_{f1m} \\ \boldsymbol{K}_{fk1} & \boldsymbol{K}_{fkl} & \cdots & \boldsymbol{K}_{fkm} \\ \vdots & \vdots & \ddots & \vdots \\ \boldsymbol{K}_{fm1} & \boldsymbol{K}_{fml} & \cdots & \boldsymbol{K}_{fmm} \end{bmatrix} \begin{bmatrix} g_{11} & g_{1j} & \cdots & g_{16} \\ g_{k1} & g_{kj} & \cdots & g_{k6} \\ \vdots & \vdots & \ddots & \vdots \\ g_{m1} & g_{mj} & \cdots & g_{m6} \end{bmatrix}, \quad (5)$$

where $i = 2, \cdots, 5$, $j = 2, \cdots, 5$, $k = 2, \cdots, m-1$, and $l = 2, \cdots, m-1$.

Next, we find the stiffness relation between the fingertip space and the joint space. It is associated with the structure of finger in the hand. For a closed-loop structured finger, the stiffness matrix ${}^i\boldsymbol{K}_f^{'}({}^in_{fp} \times {}^in_{fp})$ in the ith fingertip space including the effect of the change of joint configuration can be represented as follows[27]:

$$[{}^i\boldsymbol{K}_f^{'}] = [{}^i\boldsymbol{G}_f^q]^T[{}^i\boldsymbol{K}_q][{}^i\boldsymbol{G}_f^q] - ([{}^iT_q]^T \circ [{}^i\boldsymbol{H}_{ff}^q]), \quad (6)$$

and we define

$$[{}^i\boldsymbol{K}_f] = [{}^i\boldsymbol{K}_f^{'}] + ([{}^iT_q]^T \circ [{}^i\boldsymbol{H}_{ff}^q]) = [{}^i\boldsymbol{G}_f^q]^T[{}^i\boldsymbol{K}_q][{}^i\boldsymbol{G}_f^q], \quad (7)$$

where $[{}^i\boldsymbol{K}_q]$ represents the ${}^in_j \times {}^in_j$ stiffness matrix in the joint space of each finger, $[{}^i\boldsymbol{G}_f^q]$ denotes a Jacobian(i.e., backward mapping) relating the joint space q to the fingertip space f, and $[{}^i\boldsymbol{H}_{ff}^q]$ represents the second-order kinematic influence coefficient matrix induced by the change of joint configuration described[25], and more detail for the second-order kinematic influence coefficient matrix is described[26].

3 Independent Finger-based Compliance Control

This section describes the procedure for computing the fingertip stiffness without inter-finger coupling so as to achieve the desired stiffness in the operational space. For convenience of describing the independent finger-based compliance control, we particularly consider the case of two-fingered hand, where its contact type is assumed a point contact with friction and its workspace is confined in two-dimensional space.

When a two-fingered hand manipulates an object in the two-dimensional space as shown in Figure 2, let the desired 2×2 object stiffness matrix in the operational space be given as

$$[\boldsymbol{K}_o] = \begin{bmatrix} \boldsymbol{K}_{oxx} & \boldsymbol{K}_{oxy} \\ \boldsymbol{K}_{oyx} & \boldsymbol{K}_{oyy} \end{bmatrix}. \quad (8)$$

According to the necessary finger condition(two fingers) for stiffness control, this two-fingered system satisfies the necessary condition[21]. The 4×4 stiffness matrix in the fingertip space is generally represented by

$$[\boldsymbol{K}_f] = \left[\begin{array}{cc|cc} {}^1\boldsymbol{K}_{fxx} & {}^1\boldsymbol{K}_{fxy} & {}^{12}\boldsymbol{K}_{fxx} & {}^{12}\boldsymbol{K}_{fxy} \\ {}^1\boldsymbol{K}_{fyx} & {}^1\boldsymbol{K}_{fyy} & {}^{12}\boldsymbol{K}_{fyx} & {}^{12}\boldsymbol{K}_{fyy} \\ \hline {}^{21}\boldsymbol{K}_{fxx} & {}^{21}\boldsymbol{K}_{fxy} & {}^2\boldsymbol{K}_{fxx} & {}^2\boldsymbol{K}_{fxy} \\ {}^{21}\boldsymbol{K}_{fyx} & {}^{21}\boldsymbol{K}_{fyy} & {}^2\boldsymbol{K}_{fyx} & {}^2\boldsymbol{K}_{fyy} \end{array}\right], \quad (9)$$

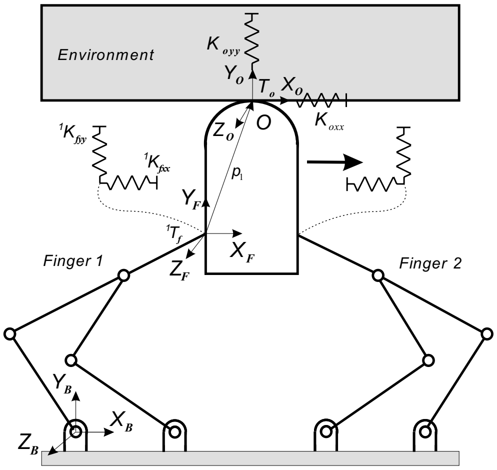

Figure 2: Compliance control by two-fingers for $\boldsymbol{K}_o(2 \times 2)$.

where the off-diagonal blocks denote the inter-finger coupling matrices, and ${}^i\boldsymbol{K}_{fxy}(i = 1, 2)$ denotes the coupling stiffness elements between the x- and y-direction in the ith fingertip space.

A grip Jacobian matrix relating the small displacement of the operational position to that of the finger positions is given by

$$\begin{bmatrix} [{}^1\boldsymbol{G}_o^f] \\ [{}^2\boldsymbol{G}_o^f] \end{bmatrix} = \begin{bmatrix} b_{11} & b_{12} \\ b_{21} & b_{22} \\ b_{31} & b_{32} \\ b_{41} & b_{42} \end{bmatrix}. \tag{10}$$

Here, our objective is to eliminate inter-finger couplings as well as the coupling of the fingertip space for effective hybrid control in the fingertip space. So, the stiffness matrix satisfying this objective is set up as below,

$$[\boldsymbol{K}_f^d] = \left[\begin{array}{cc|cc} {}^1\boldsymbol{K}_{fxx}^d & 0 & 0 & 0 \\ 0 & {}^1\boldsymbol{K}_{fyy}^d & 0 & 0 \\ \hline 0 & 0 & {}^2\boldsymbol{K}_{fxx}^d & 0 \\ 0 & 0 & 0 & {}^2\boldsymbol{K}_{fyy}^d \end{array}\right]. \tag{11}$$

where ${}^i\boldsymbol{K}_{fxx}^d$ and ${}^i\boldsymbol{K}_{fyy}^d$ denote the desired x- and y-directional stiffness elements in the fingertip space of the ith finger, respectively.

Then, the equation (4) can be rearranged as a vector form

$$K_{oo} = [\boldsymbol{B}_f^o]\ K_{ff}, \tag{12}$$

where

$$K_{oo} = \begin{bmatrix} \boldsymbol{K}_{oxx} & \boldsymbol{K}_{oxy} & \boldsymbol{K}_{oyy} \end{bmatrix}^T,$$
$$K_{ff} = \begin{bmatrix} {}^1\boldsymbol{K}_{fxx}^d & {}^1\boldsymbol{K}_{fyy}^d & {}^2\boldsymbol{K}_{fxx}^d & {}^2\boldsymbol{K}_{fyy}^d \end{bmatrix}^T,$$

and

$$[\boldsymbol{B}_f^o] = \begin{bmatrix} (b_{11})^2 & (b_{21})^2 & (b_{31})^2 & (b_{41})^2 \\ b_{11}b_{12} & b_{21}b_{22} & b_{31}b_{32} & b_{41}b_{42} \\ (b_{12})^2 & (b_{22})^2 & (b_{32})^2 & (b_{42})^2 \end{bmatrix}.$$

In the three-dimensional case, the independent stiffness relation given by (12) can be generally expressed by

$$K_{oo} = \begin{bmatrix} g_{11}^2 & g_{l1}^2 & \cdots & g_{m1}^2 \\ g_{11}g_{1i} & g_{l1}g_{li} & \cdots & g_{m1}g_{mi} \\ \vdots & \vdots & \ddots & \vdots \\ g_{11}g_{16} & g_{l1}g_{l6} & \cdots & g_{m1}g_{m6} \\ g_{12}^2 & g_{l2}^2 & \cdots & g_{m2}^2 \\ g_{12}g_{1k} & g_{l2}g_{lk} & \cdots & g_{m2}g_{mk} \\ \vdots & \vdots & \ddots & \vdots \\ g_{12}g_{16} & g_{l2}g_{l6} & \cdots & g_{m2}g_{m6} \\ \vdots & \vdots & \vdots & \vdots \\ g_{15}^2 & g_{l5}^2 & \cdots & g_{m5}^2 \\ g_{15}g_{16} & g_{l5}g_{l6} & \cdots & g_{m5}g_{m6} \\ g_{16}^2 & g_{l6}^2 & \cdots & g_{m6}^2 \end{bmatrix} K_{ff}, \tag{13}$$

where

$$K_{oo} = [\boldsymbol{K}_{o11}\ \boldsymbol{K}_{o1j}\ \cdots\ \boldsymbol{K}_{o16}\ \boldsymbol{K}_{o22}\ \cdots\ \boldsymbol{K}_{o26}$$
$$\cdots\ \boldsymbol{K}_{o66}]^T,$$
$$K_{ff} = [\boldsymbol{K}_{f11}\ \boldsymbol{K}_{fll}\ \cdots\ \boldsymbol{K}_{fmm}]^T,$$

and here $i = 2, \cdots, 5$, $j = 2, \cdots, 5$, $k = 3, \cdots, 5$, and $l = 2, \cdots, m-1$.

From (12) and (13), the structure of $[\boldsymbol{B}_f^o]$ may change according to the grasping geometry. To be specific, the sign of some elements of $[\boldsymbol{B}_f^o]$ may be changed from positive to negative or zero. Therefore, operational stiffness elements should be considerably specified in consideration of the grasp geometry.

Generally, the problem of computing the fingertip stiffness for a given operational stiffness can be transferred a linear programming problem of the form; find K_{ff} from the following linear matrix equation given by

$$K_{oo} = [\boldsymbol{B}_f^o]\ K_{ff}, \tag{14}$$

subject to $K_{ff} \geq 0$.

Consequently, we can obtain the independent finger stiffness elements K_{ff} by solving the linear programming problem given in (14).

4 Analysis of Operational Compliance Characteristics

In this section, through the observation of the stiffness relation between the operational space and the fingertip space of multi-fingered hands, we provide a guideline for specifying the operational compliance characteristics in two- and three-dimensional spaces for assembly tasks.

4.1 Two-dimensional Case

Consider a rigid peg being inserted in a hole by a three-fingered robot hand in two-dimensional space as shown in Figure 3.

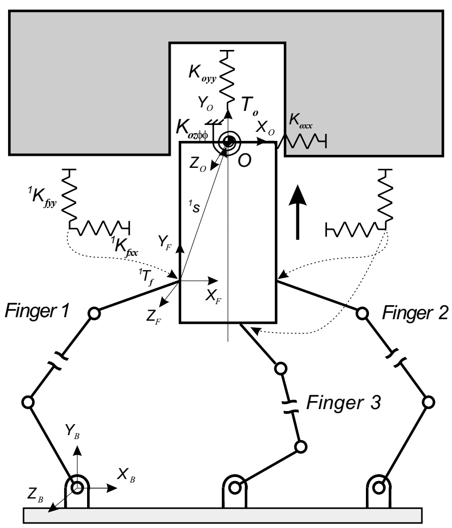

Figure 3: Peg-in-hole task using a three-fingered robot hand in two-dimensional space.

In Figure 3, the independent stiffness relation (12) between the operational space and the fingertip space is given by

$$\begin{bmatrix} \boldsymbol{K}_{oxx} \\ \boldsymbol{K}_{oxy} \\ \boldsymbol{K}_{ox\phi} \\ \boldsymbol{K}_{oyy} \\ \boldsymbol{K}_{oy\phi} \\ \boldsymbol{K}_{o\phi\phi} \end{bmatrix} = \begin{bmatrix} 1.0 & 0.0 & 1.0 & 0.0 & 1.0 & 0.0 \\ 0.0 & 0.0 & 0.0 & 0.0 & 0.0 & 0.0 \\ y_1 & 0.0 & y_2 & 0.0 & y_3 & 0.0 \\ 0.0 & 1.0 & 0.0 & 1.0 & 0.0 & 1.0 \\ 0.0 & -x_1 & 0.0 & x_2 & 0.0 & x_3 \\ y_1^2 & x_1^2 & y_2^2 & x_2^2 & y_3^2 & x_3^2 \end{bmatrix} \begin{bmatrix} {}^1\boldsymbol{K}_{fxx} \\ {}^1\boldsymbol{K}_{fyy} \\ {}^2\boldsymbol{K}_{fxx} \\ {}^2\boldsymbol{K}_{fyy} \\ {}^3\boldsymbol{K}_{fxx} \\ {}^3\boldsymbol{K}_{fyy} \end{bmatrix}, \tag{15}$$

where x_i and y_i denote the elements of position vectors directing from the ith finger contact position to the task position, and they are given to be all positive. $[{}^i\boldsymbol{K}_{fxx}]$ and $[{}^i\boldsymbol{K}_{fyy}]$ represent the x- and y-directional stiffness elements in the fingertip space of the ith finger, respectively.

Note that the elements of the second row of the mapping matrix $[\boldsymbol{B}_f^o]$ in (15) are calculated as zero. This is because we excluded the coupling terms ${}^i\boldsymbol{K}_{fxy}(i=1,2,3)$ in the fingertip space for independent compliance control. Thus, we have zero $\boldsymbol{K}_{oxy}$, which, in fact, is a linear combination of ${}^i\boldsymbol{K}_{fxy}(i=1,2,3)$. Also, note that the third row of $[\boldsymbol{B}_f^o]$ corresponds to modulation of $\boldsymbol{K}_{ox\phi}$. However, we can easily notice that zero $\boldsymbol{K}_{ox\phi}$ cannot be achieved. This is because the components of K_{ff} are always positive and the three influence coefficients(i.e., y_1, y_2, and y_3) are always positive in this grasped configuration.

Consequently, the stiffness matrix in the operational space can be specified as follows:

$$\begin{bmatrix} \boldsymbol{K}_{oxx} & \boldsymbol{K}_{oxy} & \boldsymbol{K}_{ox\phi} \\ \boldsymbol{K}_{oyx} & \boldsymbol{K}_{oyy} & \boldsymbol{K}_{oy\phi} \\ \boldsymbol{K}_{o\phi x} & \boldsymbol{K}_{o\phi y} & \boldsymbol{K}_{o\phi\phi} \end{bmatrix} = \begin{bmatrix} S & 0 & +\psi_1 \\ 0 & L & 0, \pm\psi_2 \\ +\psi_1 & 0, \pm\psi_2 & S \end{bmatrix}, \tag{16}$$

where ψ_1 and ψ_2 are all positive parameters. And S and L mean that small and large value of stiffness, respectively. The diagonal elements can be determined by considering the task characteristic for each direction[22]-[24].

In (16), ψ_2 can be arbitrarily planned according to the given task, but ψ_1 cannot be arbitrarily planned. Thus, ψ_1 is determined by the following procedure. Let $[\boldsymbol{D}_f^o]$ be the matrix excluding the second and third rows of $[\boldsymbol{B}_f^o]$ and K_{oo}^* be the vector excluding $\boldsymbol{K}_{oxy}$ and $\boldsymbol{K}_{ox\phi}$ of K_{oo}. Then, K_{ff} can be obtained by solving the following linear matrix equation:

$$K_{oo}^* = [\boldsymbol{D}_f^o] K_{ff} \tag{17}$$

subject to $K_{ff} \geq 0$.

Then, the coupling stiffness element ψ_1 can be determined by

$$\psi_1 = [\boldsymbol{B}_f^o]_3 \; K_{ff}, \tag{18}$$

where $[\boldsymbol{B}_f^o]_i$ denotes the ith row of $[\boldsymbol{B}_f^o]$.

4.2 Three-dimensional Case

Next, consider a peg-in-hole task in three-dimensional space as shown in Figure 4.

In Figure 4, the independent stiffness relation between the operational space and the fingertip space is given by

$$
\begin{aligned}
K_{oo} &= [\boldsymbol{B}_f^o]\, K_{ff} \\
\begin{bmatrix} \boldsymbol{K}_{oxx} \\ \boldsymbol{K}_{oxy} \\ \boldsymbol{K}_{oxz} \\ \boldsymbol{K}_{ox\gamma} \\ \boldsymbol{K}_{ox\beta} \\ \boldsymbol{K}_{ox\alpha} \\ \boldsymbol{K}_{oyy} \\ \boldsymbol{K}_{oyz} \\ \boldsymbol{K}_{oy\gamma} \\ \boldsymbol{K}_{oy\beta} \\ \boldsymbol{K}_{oy\alpha} \\ \boldsymbol{K}_{ozz} \\ \boldsymbol{K}_{oz\gamma} \\ \boldsymbol{K}_{oz\beta} \\ \boldsymbol{K}_{oz\alpha} \\ \boldsymbol{K}_{o\gamma\gamma} \\ \boldsymbol{K}_{o\gamma\beta} \\ \boldsymbol{K}_{o\gamma\alpha} \\ \boldsymbol{K}_{o\beta\beta} \\ \boldsymbol{K}_{o\beta\alpha} \\ \boldsymbol{K}_{o\alpha\alpha} \end{bmatrix}
&= \left[\begin{array}{cccccccccccc}
1 & 0 & 0 & 1 & 0 & 0 & 1 & 0 & 0 & 1 & 0 & 0 \\
0 & 0 & 0 & 0 & 0 & 0 & 0 & 0 & 0 & 0 & 0 & 0 \\
0 & 0 & 0 & 0 & 0 & 0 & 0 & 0 & 0 & 0 & 0 & 0 \\
0 & 0 & 0 & 0 & 0 & 0 & 0 & 0 & 0 & 0 & 0 & 0 \\
-z_1 & 0 & 0 & -z_2 & 0 & 0 & -z_3 & 0 & 0 & -z_4 & 0 & 0 \\ \hline
-y_1 & 0 & 0 & y_2 & 0 & 0 & -y_3 & 0 & 0 & y_4 & 0 & 0 \\
0 & 1 & 0 & 0 & 1 & 0 & 0 & 1 & 0 & 0 & 1 & 0 \\
0 & 0 & 0 & 0 & 0 & 0 & 0 & 0 & 0 & 0 & 0 & 0 \\
0 & z_1 & 0 & 0 & z_2 & 0 & 0 & z_3 & 0 & 0 & z_4 & 0 \\ \hline
0 & 0 & 0 & 0 & 0 & 0 & 0 & 0 & 0 & 0 & 0 & 0 \\
0 & -x_1 & 0 & 0 & x_2 & 0 & 0 & x_3 & 0 & 0 & -x_4 & 0 \\
0 & 0 & 1 & 0 & 0 & 1 & 0 & 0 & 1 & 0 & 0 & 1 \\
0 & 0 & y_1 & 0 & 0 & -y_2 & 0 & 0 & y_3 & 0 & 0 & -y_4 \\
0 & 0 & x_1 & 0 & 0 & -x_2 & 0 & 0 & -x_3 & 0 & 0 & x_4 \\
0 & 0 & 0 & 0 & 0 & 0 & 0 & 0 & 0 & 0 & 0 & 0 \\
0 & z_1^2 & y_1^2 & 0 & z_2^2 & y_2^2 & 0 & z_3^2 & y_3^2 & 0 & z_4^2 & y_4^2 \\
0 & 0 & x_1y_1 & 0 & 0 & x_2y_2 & 0 & 0 & -x_3y_3 & 0 & 0 & -x_4y_4 \\
0 & -x_1z_1 & 0 & 0 & x_2z_2 & 0 & 0 & x_3z_3 & 0 & 0 & -x_4z_4 & 0 \\
z_1^2 & 0 & x_1^2 & z_2^2 & 0 & x_2^2 & z_3^2 & 0 & x_3^2 & z_4^2 & 0 & x_4^2 \\
y_1z_1 & 0 & 0 & -y_2z_2 & 0 & 0 & y_3z_3 & 0 & 0 & -y_4z_4 & 0 & 0 \\
y_1^2 & x_1^2 & 0 & y_2^2 & x_2^2 & 0 & y_3^2 & x_3^2 & 0 & y_4^2 & x_4^2 & 0
\end{array} \right. \\
&\qquad \left. \begin{array}{ccccccccc}
1 & 0 & 0 & 1 & 0 & 0 & 1 & 0 & 0 \\
0 & 0 & 0 & 0 & 0 & 0 & 0 & 0 & 0 \\
0 & 0 & 0 & 0 & 0 & 0 & 0 & 0 & 0 \\
0 & 0 & 0 & 0 & 0 & 0 & 0 & 0 & 0 \\
-z_5 & 0 & 0 & -z_6 & 0 & 0 & -z_7 & 0 & 0 \\ \hline
-y_5 & 0 & 0 & y_6 & 0 & 0 & -y_7 & 0 & 0 \\
0 & 1 & 0 & 0 & 1 & 0 & 0 & 1 & 0 \\
0 & 0 & 0 & 0 & 0 & 0 & 0 & 0 & 0 \\
0 & z_5 & 0 & 0 & z_6 & 0 & 0 & z_7 & 0 \\ \hline
0 & 0 & 0 & 0 & 0 & 0 & 0 & 0 & 0 \\
0 & x_5 & 0 & 0 & x_6 & 0 & 0 & x_7 & 0 \\
0 & 0 & 1 & 0 & 0 & 1 & 0 & 0 & 1 \\
0 & 0 & y_5 & 0 & 0 & -y_6 & 0 & 0 & y_7 \\
0 & 0 & -x_5 & 0 & 0 & x_6 & 0 & 0 & -x_7 \\
0 & 0 & 0 & 0 & 0 & 0 & 0 & 0 & 0 \\
0 & z_5^2 & y_5^2 & 0 & z_6^2 & y_6^2 & 0 & z_7^2 & y_7^2 \\
0 & 0 & -x_5y_5 & 0 & 0 & -x_6y_6 & 0 & 0 & -x_7y_7 \\
0 & x_5z_5 & 0 & 0 & -x_6z_6 & 0 & 0 & x_7z_7 & 0 \\
z_5^2 & 0 & x_5^2 & z_6^2 & 0 & x_6^2 & z_7^2 & 0 & x_7^2 \\
y_5z_5 & 0 & 0 & -y_6z_6 & 0 & 0 & y_7z_7 & 0 & 0 \\
y_5^2 & x_5^2 & 0 & y_6^2 & x_6^2 & 0 & y_7^2 & x_7^2 & 0
\end{array} \right]
\begin{bmatrix} {}^1\boldsymbol{K}_{fxx} \\ {}^1\boldsymbol{K}_{fyy} \\ {}^1\boldsymbol{K}_{fzz} \\ {}^2\boldsymbol{K}_{fxx} \\ {}^2\boldsymbol{K}_{fyy} \\ {}^2\boldsymbol{K}_{fzz} \\ {}^3\boldsymbol{K}_{fxx} \\ {}^3\boldsymbol{K}_{fyy} \\ {}^3\boldsymbol{K}_{fzz} \\ {}^4\boldsymbol{K}_{fxx} \\ {}^4\boldsymbol{K}_{fyy} \\ {}^4\boldsymbol{K}_{fzz} \\ {}^5\boldsymbol{K}_{fxx} \\ {}^5\boldsymbol{K}_{fyy} \\ {}^5\boldsymbol{K}_{fzz} \\ {}^6\boldsymbol{K}_{fxx} \\ {}^6\boldsymbol{K}_{fyy} \\ {}^6\boldsymbol{K}_{fzz} \\ {}^7\boldsymbol{K}_{fxx} \\ {}^7\boldsymbol{K}_{fyy} \\ {}^7\boldsymbol{K}_{fzz} \end{bmatrix}, \quad (19)
\end{aligned}
$$

where x_i, y_i, and z_i denote the elements of position vectors directing from the ith finger contact position to the task position, and they are given to be all positive. $[{}^i\boldsymbol{K}_{fxx}]$, $[{}^i\boldsymbol{K}_{fyy}]$, and $[{}^i\boldsymbol{K}_{fzz}]$ represent the x-, y-, and z-directional stiffness elements in the fingertip space of the ith finger, respectively.

Note that the elements of the $[\boldsymbol{B}_f^o]_2$, $[\boldsymbol{B}_f^o]_3$, $[\boldsymbol{B}_f^o]_4$, $[\boldsymbol{B}_f^o]_8$, $[\boldsymbol{B}_f^o]_{10}$, and $[\boldsymbol{B}_f^o]_{15}$ in (19) are shown zero. This is because we excluded the coupling terms(${}^i\boldsymbol{K}_{fxy}$, ${}^i\boldsymbol{K}_{fxz}$, and ${}^i\boldsymbol{K}_{fyz}(i = 1, 2, \cdots, 7)$) in the fingertip space for independent compliance control.

Thus, we have zero $\boldsymbol{K}_{oxy}$, $\boldsymbol{K}_{oxz}$, $\boldsymbol{K}_{ox\gamma}$, $\boldsymbol{K}_{oyz}$, $\boldsymbol{K}_{oy\beta}$, and $\boldsymbol{K}_{oz\alpha}$, which, in fact, is a linear combination of ${}^i\boldsymbol{K}_{fxy}$, ${}^i\boldsymbol{K}_{fxz}$, and ${}^i\boldsymbol{K}_{fyz}$ for $i = 1, 2, \cdots, 7$.

Also, note that the 5th row of $[\boldsymbol{B}_f^o]$ corresponds to the modulation of $\boldsymbol{K}_{ox\beta}$ and the 9th row of $[\boldsymbol{B}_f^o]$ corresponds to the modulation of $\boldsymbol{K}_{oy\gamma}$. However, we can easily notice that zero $\boldsymbol{K}_{ox\beta}$ and $\boldsymbol{K}_{ox\gamma}$ cannot be achieved by all positive stiffness components K_{ff}

defined in the fingertip space and positive influence coefficients (i.e., $z_i(i = 1, 2, \cdots, 7)$) in this grasp configuration.

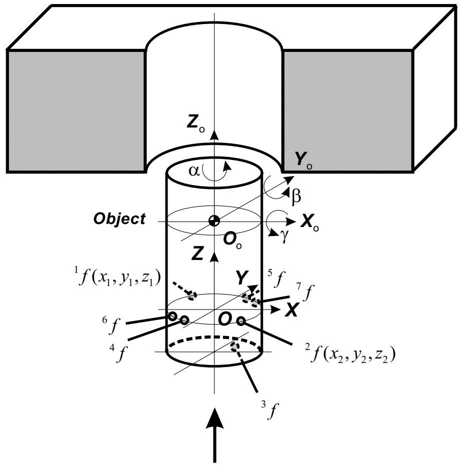

Figure 4: Peg-in-hole task using a seven-fingered hand in three-dimensional space.

Consequently, the stiffness matrix in the operational space can be specified as follows:

$$\begin{bmatrix} \boldsymbol{K}_{oxx} & \boldsymbol{K}_{oxy} & \boldsymbol{K}_{oxz} & \boldsymbol{K}_{ox\gamma} & \boldsymbol{K}_{ox\beta} & \boldsymbol{K}_{ox\alpha} \\ \boldsymbol{K}_{oyx} & \boldsymbol{K}_{oyy} & \boldsymbol{K}_{oyz} & \boldsymbol{K}_{oy\gamma} & \boldsymbol{K}_{oy\beta} & \boldsymbol{K}_{oy\alpha} \\ \boldsymbol{K}_{ozx} & \boldsymbol{K}_{ozy} & \boldsymbol{K}_{ozz} & \boldsymbol{K}_{oz\gamma} & \boldsymbol{K}_{oz\beta} & \boldsymbol{K}_{oz\alpha} \\ \boldsymbol{K}_{o\gamma x} & \boldsymbol{K}_{o\gamma y} & \boldsymbol{K}_{o\gamma z} & \boldsymbol{K}_{o\gamma\gamma} & \boldsymbol{K}_{o\gamma\beta} & \boldsymbol{K}_{o\gamma\alpha} \\ \boldsymbol{K}_{o\beta x} & \boldsymbol{K}_{o\beta y} & \boldsymbol{K}_{o\beta z} & \boldsymbol{K}_{o\beta\gamma} & \boldsymbol{K}_{o\beta\beta} & \boldsymbol{K}_{o\beta\alpha} \\ \boldsymbol{K}_{o\alpha x} & \boldsymbol{K}_{o\alpha y} & \boldsymbol{K}_{o\alpha z} & \boldsymbol{K}_{o\alpha\gamma} & \boldsymbol{K}_{o\alpha\beta} & \boldsymbol{K}_{o\alpha\alpha} \end{bmatrix} =$$

$$\begin{bmatrix} S & 0 & 0 & 0 & -\psi_1 & 0, \pm\psi_2 \\ 0 & S & 0 & +\psi_3 & 0 & 0, \pm\psi_4 \\ 0 & 0 & L & 0, \pm\psi_5 & 0, \pm\psi_6 & 0 \\ 0 & +\psi_3 & 0, \pm\psi_5 & S & 0, \pm\psi_7 & 0, \pm\psi_8 \\ -\psi_1 & 0 & 0, \pm\psi_6 & 0, \pm\psi_7 & S & 0, \pm\psi_9 \\ 0, \pm\psi_2 & 0, \pm\psi_4 & 0 & 0, \pm\psi_8 & 0, \pm\psi_9 & L \end{bmatrix} \tag{20}$$

where $\psi_i(i = 1, 2, \cdots, 9)$ are all positive parameters.

In (20), ψ_2 and $\psi_i(i = 4, \cdots, 9)$ can be arbitrarily determined and also those parameters can be suitably adjusted by considering additional control performance(e.g. the jamming effect of assembly tasks). On the other hand, ψ_1 and ψ_3 corresponding to $\boldsymbol{K}_{ox\beta}$ and $\boldsymbol{K}_{oy\gamma}$, respectively, cannot be arbitrarily planned according to the previous analysis. Thus, they are determined by the following procedure. Let $[\boldsymbol{D}_f^o](13 \times 21)$ be the matrix excluding the $[\boldsymbol{B}_f^o]_2$, $[\boldsymbol{B}_f^o]_3$, $[\boldsymbol{B}_f^o]_4$, $[\boldsymbol{B}_f^o]_5$, $[\boldsymbol{B}_f^o]_8$, $[\boldsymbol{B}_f^o]_9$, $[\boldsymbol{B}_f^o]_{10}$, and $[\boldsymbol{B}_f^o]_{15}$ and K_{oo}^* in (19), and $K_{oo}^*(13 \times 1)$ be the vector excluding $\boldsymbol{K}_{oxy}$, $\boldsymbol{K}_{oxz}$, $\boldsymbol{K}_{ox\gamma}$, $\boldsymbol{K}_{ox\beta}$, $\boldsymbol{K}_{oyz}$, $\boldsymbol{K}_{oy\gamma}$, $\boldsymbol{K}_{oy\beta}$, and $\boldsymbol{K}_{oz\alpha}$ of K_{oo}. Then, K_{ff} can be obtained by solving the following linear matrix equation:

$$K_{oo}^* = [\boldsymbol{D}_f^o] K_{ff}. \tag{21}$$

subject to $K_{ff} \geq 0$.

Then, the coupling stiffness element ψ_1 and ψ_3 can be determined by

$$\psi_1 = -[\boldsymbol{B}_f^o]_5 \; K_{ff}, \tag{22}$$

$$\psi_3 = [\boldsymbol{B}_f^o]_9 \; K_{ff}, \tag{23}$$

where $[\boldsymbol{B}_f^o]_i$ denotes the ith row of $[\boldsymbol{B}_f^o]$.

In typical assembly tasks, the RCC(Remote Compliance Center) point exists at the distal position of the peg as shown in Figure 4. However, if the RCC point lies inside the polygon formed by the finger contact point, the coupling stiffness elements(i.e., $\boldsymbol{K}_{ox\beta}$ and $\boldsymbol{K}_{oy\gamma}$) can be made zero since some of the kinematic influence coefficients of the 5th and 9th rows of (19) change their signs.

Assuming a point contact with friction, a multi-fingered hand should have at least seven fingers to modulate 6×6 operational stiffness characteristic in three-dimensional space[21], since the operational stiffness matrix has 21 independent stiffness elements. However, as the above-mentioned, the independent compliance control of a multi-fingered hand provides us with partially decoupled compliance characteristics in the operational space. According to (19), the number of the independent compliance elements are fifteen. Thus, we can confirm that the six-degree of freedom compliance control can be achievable with a five-fingered hand. This result is somewhat exiting in that human hand has five fingers.

5 Concluding Remarks

A guideline for specifying compliance characteristics in the operational space of multi-fingered hands was analyzed in this paper. Through analyzing the stiffness relation between the operational space and the fingertip space of multi-fingered hands, it is shown that some of coupling stiffness elements cannot be planned arbitrary. As a result, we showed that a five-fingered hand is necessary to modulate 6×6 operational stiffness matrix by using an independent finger-based compliance control method. Also, we can notice that the operational stiffness matrix should be carefully specified in consideration the grasp geometry of multi-fingered hands for successful grasping and manipulation tasks.

Companion paper presents task-based guideline for specifying compliance characteristics of multi-fingered hands.

References

[1] H. Hashmoto, H. Ogawa, M. Obama, T. Umeda, K. Tatuno, and T. Furukawa, "Development of a multi-fingered robot hand with fingertip tactile sensors," *Proc. of IEEE Int. Conf. on Intelligent Robots and Systems*, pp. 875-882, 1993.

[2] H. Maekawa, K. Komoria, and K. Tanie, "Manipulation of an unknown object by multifingered hands with rolling contact using tactile feedback," *Proc. of IEEE/RSJ Int. Conf. on Intelligent Robots and Systems*, pp. 1877-1882, July 1992.

[3] T. Yoshikawa, and X. -Z. Zheng, "Coordinated dynamic hybrid position/force control for multiple robot manipulators handling one constrained object," *Int. Jour. of Robotics Research*, Vol. 12, No. 3, pp. 219-230, 1993.

[4] H. Maekawa, K. Tanie, and K. Komoria, "Tactile sensor based manipulation of an unknown object by a multifingered hand with rolling contact," *Proc. of IEEE Int. Conf. on Robotics and Automation*, pp. 743-750, May 1995.

[5] T. Hasegawa, T. Matsuoka, T. Kiriki, and K, Honda, "Manipulation of an object by a multi-fingered hand with multi-sensors," *Proc. of Int. Conf. on Industrial Electronics, Control, and Instrumentation*, pp. 174-179, 1996.

[6] H. Maekawa, K. Tanie, and K. Komoria, "Dynamic grasping force control using tactile feedback for grasp of multifingered hand," *Proc. of IEEE Int. Conf. on Robotics and Automation*, pp. 2462-2469, April 1996.

[7] K. J. Kyriakopoulos, J. V. Riper, A. Zink, and H. E. Stepanou, "Kinematic analysis and position/force control of the Anthrobot dextrous hand," *IEEE Trans. on System, Man, and Cybernetics-Part B: Cybernetics*, Vol. 27, No. 1, pp. 95-104, Feb. 1997.

[8] S. L. Jiang, K. K. Choi, and Z. X. Li, "Coordinated motion generation for multifingered manipulation using tactile feedback," *Proc. of IEEE Int. Conf. on Robotics and Automation*, pp. 3032-3037, May 1999.

[9] J. L. Pons, R. Ceres, and F, Pfeiffer, "Multifingered dexterous robotics hand design and control: a review," *Robotica*, Vol. 17, pp. 661-674, 1999.

[10] M. R. Cutkosky, and I. Kao, "Computing and controlling the compliance of a robotic hand," *IEEE Trans. on Robotics and Automation*, Vol. 5, No. 2, pp. 151-165, 1989.

[11] I. Kao, M. R. Cutkosky, and R. S. Johansson, "Robotic stiffness control and calibration as applied to humnan grasping tasks," *IEEE Trans. on Robotics and Automation*, Vol. 13, No. 4, pp. 557-566, 1997.

[12] D. E. Whitney, "Quasi-static assembly of compliantly supported rigid parts," *Jour. of Dynamic systems, Measurement, and control*, Vol. 104, pp. 65-77, March 1982.

[13] H. Asada, Y. Kakumoto, "The dynamic analysis and design of a high-speed insertion hand using the generalized centroid and virtual mass," *Jour. of Dynamic systems, Measurement, and control*, Vol. 112, pp. 646-652, 1990.

[14] T. Matsuoka, T. Hasegawa, T. Kiriki, and K, Honda, "Mechanical assembly based on motion primitives of multi-fingered hand," *Proc. of Advanced Intelligent Mechatronics*, 1997.

[15] K. B. Shimoga, "Robot grasp synthesis algorithms: a survey," *Int. Jour. of Robotics Research*, Vol. 15, No. 3, pp. 230-266, 1996.

[16] V. Nguyen, "Constructing force-closure grasps in 3-D," *Proc. of IEEE Int. Conf. on Robotics and Automation*, pp. 240-245, March 1987.

[17] K. Yokoi, M. Kaneko, and K. Tanie, "A compliance control method suggested by muscle networks in human arms," *Proc. of IEEE/RSJ Int. Conf. on Intelligent Robots and Systems*, pp. 385-390, 1988.

[18] M. H. Ang, Jr. and G. B. Andeen, "Specifying and achieving passive compliance based on manipulator structure," *IEEE Trans. on Robotics and Automation*, Vol. 11, No. 4, pp. 504-515, 1995.

[19] J. Li and I. Kao, "Grasp stiffness matrix – fundanmental properties in analysis of grasping and manipulation," *Proc. of IEEE/RSJ Int. Conf. on Intelligent Robots and Systems*, pp. 381-386, 1995.

[20] G. P, Starr, "An experimental investigation of object stiffness control using multifingered hand," *Robotics and Autonomous Systems*, no. 10, pp. 33-42, 1992.

[21] B. -H. Kim, B. -J. Yi, I. H. Suh, and S. -R. Oh, "A biomimetic compliance control of robot hand by considering structures of human finger," *Proc. of IEEE Int. Conf. on Robotics and Automation*, pp. 3880-3887, 2000.

[22] J. D. Schutter and H. V. Brussel, "Compliant robot motion I. A formalism for specifying compliant motion tasks," *Int. Jour. of Robotics Research*, vol. 7, no. 4, pp. 3-17, 1988.

[23] J. D. Schutter and H. V. Brussel, "Compliant robot motion II. A control approach based on external control loops," *Int. Jour. of Robotics Research*, vol. 7, no. 4, pp. 18-33, 1988.

[24] K. B. Shimoga and A. A. Goldenberg, "Grasp admittance center: choosing admittance center parameters," *Proc. of American Control Conference*, pp. 2527-2532, 1991.

[25] R. A. Freeman and D. Tesar, "Dynamic modeling of serial and parallel mechanisms/robotics systems, Part I-methodology, Part II-applications," *Proc. 20th ASME Biennial Mechanisms Conf. Orlando, FL, Trends and Development in Mechanisms, Machines, and Robotics,* DE-Vol. 15-2, pp. 7-21, 1988.

[26] B. -J. Yi, I. D. Walker, D. Tesar, and R. A. Freeman, "Geometric stability in force control," *Proc. of IEEE Int. Conf. on Robotics and Automation*, pp.281-286, 1991.

[27] B. -R. So, B. -J. Yi, S. -R. Oh, and I. H. Suh, "An independent joint-based compliance control method for a five-bar finger mechanism via redundant actuators," *Proc. of IEEE Int. Conf. on Robotics and Automation*, pp. 2140-2146, 1999.